

## Original article

USING POTASSIUM FERROCYANIDE AS A SALT INHIBITOR FOR MURAL PAINTINGS:  
CHALLENGE AND EFFECTIVENESS

El Hagrassy, A.

Conservation dept., Faculty of Archaeology, Fayoum Univ., Fayoum, Egypt.

\*E-mail address: [afa01@fayoum.edu.eg](mailto:afa01@fayoum.edu.eg)

## Article info.

## Article history:

Received: 7-1-2024

Accepted: 9-9-2024

Doi: 10.21608/ejars.2025.434897

## Keywords:

Potassium Ferrocyanide

Salt inhibitors

Mural paintings

Halite

Pigments.

EJARS – Vol. 15 (1) – June 2025: 19-26

## Abstract:

The objective of this study is to regulate the process of salt crystallization that commonly occurs on cultural heritage structures, stones, and mural paintings. Halite, the predominant salt present in Egypt, has caused damage to the historical building. Managing soluble salt is a global concern for conservators, especially when it is not possible to eliminate the source of salt. Salt inhibitors are chemical compounds that are now used to regulate and impede crystallization breakdown. The study's goals were to control the crystallization of salt, find out how well and whether potassium ferrocyanide works as a salt inhibitor, and look into the possibility of using potassium ferrocyanide for painting murals in an ancient Egyptian tomb. The painted layer was identified using XRD, FTIR, and SEM-EDX techniques. The data demonstrated the combination of Egyptian blue, hematite, goethite, and malachite with egg yolk as a binding medium. The characterization analysis was employed to create replicas, apply salt inhibitors, and evaluate their effects. Different concentrations were examined to determine the effectiveness and optimal dosage for the painted layer (0.01 M, 0.1 M, and 1 M). The results showed that potassium ferrocyanide can effectively control the process of sodium chloride (NaCl) crystallization at different concentrations. The first application of potassium ferrocyanide (1M) had noticeable effects on both Egyptian blue and malachite, resulting in a darkening effect. However, the application of other concentrations yielded an acceptable result. The results indicate that the potassium ferrocyanide is effective, there is no significant color change in low concentration, and it is a highly promising agent for controlling sodium chloride crystallization in mural paintings.

## 1. Introduction

Salt crystallization greatly influences the weathering of porous building materials and mural paintings [1,2]. Salt decay is a common occurrence in historical buildings due to their long-term exposure to moisture and temperatures, which leads to salt crystallization [3]. This phenomenon caused decay in stones, plasters, and ground layers of mural paintings due to multiple factors. First, sodium chloride, a common mineral salt in Egyptian soil, is present in high levels. Second, the evaporation surface, consisting of stones, ground layers, and plasters, is the site where salt collects as a result of evaporation. Thirdly, the distribution of pore sizes typically exhibits two distinct modes, consisting of coarse pores and fine pores. It is believed that this bimodal distribution has a detrimental effect on the resistance to salt degradation [4]. Finally, because of their low mechanical strength, ground layers, plasters, and pigments are not strong enough to withstand salt crystallization pressures [5]. The interaction of salt with environmental conditions such as temperature and humidity is mainly responsible for the decay in porous stone surfaces and mural painting layers [6]. The salts can crystallize, hydrate, or dehydrate depending on the climatic conditions [7]. Salt attacks cause various

types of visible damage to stone, such as scaling, flaking, spalling, and granular disintegration [8,9]. Sodium chloride and sodium nitrate help to promote the growth of *Trichoderma spp.* in Nefer Bou Betah tomb. [10]. Numerous strategies have been employed previously; nevertheless, regulating environmental conditions is impractical in open spaces [8]. Techniques such as dry brushing, water bath treatments, or poulticing (desalination) can eliminate salts from the substrate [11,12]. Electromigration has varying degrees of efficacy. [13]. Sacrificial renders, often composed of cement and/or possessing hydrophobic qualities, are employed to collect and transmit salts from the porous archaeological stone. The primary objectives of these renders are to augment the mechanical strength of the mortar and to impede the migration of salts to the surface. However, this technique becomes challenging to use when it comes to mural paintings or painted stone surfaces [14-16]. Nonetheless, the mortars frequently lack compatibility with the existing historic material and can further cause damage [17,18]. Discovering novel methodologies is essential, as existing strategies could be unsuccessful or too costly. A new subject for investigation is the application of salt crystallization inhibitors. Desalination improvements and the reduction of

the aggressiveness and damage potential of salt weathering regimes have sparked interest. There is still a lack of basic knowledge about how additives interact with salts in stone monuments and how it affects stone deterioration processes [19]. Crystallization inhibitors have been recommended as a possible preventive treatment method for salt damage control. Nucleation onset can be prevented or delayed by these inhibitors by adsorbing onto specific crystal faces, which can alter the crystal growth mechanism [20,21]. Their activity as nucleation inhibitors remains unclear; alterations in morphology may result from either a general modification in growth mechanisms at high supersaturation or their participation as growth inhibitors. Halite crystals can be modified by preferential adsorption on specific facets or by showing dual behavior [22, 23]. Various studies have reported the use of these inhibitors, Polyphosphates and phosphates are utilized to control the formation and deposition of calcium carbonate and calcium sulfate scales, or to prevent gypsum from crystallizing spontaneously [24]. Ferrocyanide has an effect on the crystal habit of sodium chloride. The growth of sodium chloride crystals crystallizes dendrally instead of cubically (as nature dictates) [11,25]. The inhibitor's solution increases delays in blocking pores due to the longer presence of salt in solution rather than typical salt crystallization. The salt solutions were transported to the stone's surface via efflorescence instead of through damaging sub-fluorescence [25]. The behavior of efflorescence crystals that are dendritic in the presence of an inhibitor is different from the behavior of cubic crystals. Compact efflorescence is visible on the stone surface without an inhibitor and adheres poorly because it produces a larger evaporation surface, this enhances the movement of salt solution towards the surface [26]. Regarding the potentially significant inhibitory effects of ferrocyanide ions (FC) on NaCl crystallization [26], the efficacy of sodium and potassium ferrocyanides was investigated in mitigating the harm caused by sodium chloride crystallization in porous materials. The evaporation rate of the solution was measured when sodium and potassium ferrocyanides were introduced individually at concentrations ranging from 0.01 percent to 0.1 percent to a NaCl saturated solution. The additions caused the solution to move by capillary rise [22]. In another study, the impact of 0.001 M diethylene triaminepentakis methylphosphonic acid (DTPMP) and sodium ferrocyanide on 10 wt% sodium sulfate and sodium chloride solutions was examined in three different materials: Granada limestone, Czech sandstone, and fired-clay brick. They specifically investigated the salt inhibition effects of these substances. The effectiveness of DTPMP in enhancing the transportation of salt solution was greatly influenced by the substance to which it was applied. The sodium ferrocyanide was found to enhance the transport of NaCl solution in both Spanish limestone and fired-clay brick when provided at a concentration of 0.001 M but not effected on sandstone [26]. The inhibition of NaCl and KCl crystallization is attributed to ferrocyanide ions ( $[\text{Fe}(\text{CN})_6]_4^-$ ). The chloride ion ( $\text{Cl}^-$ ) that is present on the surface of NaCl and KCl is replaced by this substance, in this instance, a cyanide group is substituted for the chloride ion ( $\text{Cl}^-$ ). The different ion charge results in blocking any further growth when potassium chloride lumps are replaced on the surface [28]. This study aims to assess the effectiveness of potassium ferrocyanide as a salt inhibitor

for ancient mural paintings. Analyze the effect of their influence on both the binding media and mineral pigments. Field observation showed two principal deteriorating phenomena in the painted layer, with the initial occurrence being the loss of the painted layer and the crystallization of salt due to alternating cycles of moisture and dryness influenced by temperature and humidity. fig. (1).



**Figure (1)** the deteriorated phenomena effected the Mural Paintings of Emry tomb.

## 2. Material and Methods

### 2.1. Materials

- a) **Potassium ferrocyanide** [ $\text{K}_3\text{Fe}(\text{CN})_6$ ]: manufactured in Sigma Aldrich,  $\geq 99\%$ , Cas no: 13746-66-2, Molecular weight: 329.24.
- b) **Sodium chloride**: manufactured in pioneer for chemicals (Piochem), Egypt.
- c) **Ethyl Alcohol** (EtOH): manufactured in pioneer for chemicals (Piochem), Egypt. Assay 95%, Cas no: 64-17-5
- d) **Distilled water**: manufactured in pioneer for chemicals (Piochem), Egypt.
- e) **Paraffin wax**: El Pharanaa Company, Egypt.

### 2.2. Methods

#### 2.2.1. Experimental procedure

The experimental procedures are conducted for the first time by the author himself. The replicas were created by combining gypsum, calcite, and quartz in a ratio of 3:2:1. They are typically cast with a thickness of 5 cm on the exterior wall of the stone tomb. Filter paper is used as a barrier between the stone and the plaster. The paper facilitates the removal of replicas from the substrate. However, by allowing moisture to pass through the mortar and stone, it creates a realistic level of porosity and pore size in the mortar specimens (Replica). Subsequently, the replica was cut into dimensions of 5cm. Potassium ferrocyanide was applied by two methodologies:

- a. Injected into the painted layer at concentrations of 0.01M, 0.1M, and 1M, respectively (molar mass (329.24) \* the concentration we want to create dissolved in 1L of distilled water).
- b. By brush technique over the painted layer. 400 ml of solution is created by dissolving 5 moles of NaCl (molar mass 58.44 g/mol) in 1 liter of distilled water, with weight being the determining factor for the concentrations. The 5 cm<sup>3</sup> mural painting was placed in an upright position in the center of the dish. The molten household paraffin wax was used to seal the system and retain the mural painting, which prevented water loss through the replica. The initial weight of the setup was measured after the wax was poured. In a laboratory with good ventilation, the experiment's components were placed on a bench and kept at 40-45% relative

humidity according to the RH inside the tomb, which was taken for a year by a data logger, tab. (1).

**Table (1)** the temperature and relative humidity inside the Amry tomb, 2023

Months	Temperature °C	R.H. %
January- March	22.7	43.5
April- May	25.9	42.6
June- August	38.9	40.3
September- October	30.6	41.5
November-December	19.8	44.2

As the solution ascends through the replica, water is completely lost due to evaporation from the surfaces. We measured the flow rate through and out of the replica by weighing the setup over a period of four days, documenting visual estimations and the reduction in solution level. Documentation of the described studies was conducted approximately twice a week. The setups were photographed to obtain information about replica damage, efflorescence salt appearance, and distribution. Eventually, the replica was then removed, and the emerging salts were scraped off, collected, and weighed. Estimating the increase in weight over its initial value was used to estimate the weight of salts that were still present in the dried replica. The replicas were dried at 38 °C to recreate the actual conditions in the tomb. Periodically during the drying process, the weights of the samples were measured. The drying process involved periodically taking photos to document the efflorescence on the samples that developed. At the conclusion of the drying process, the efflorescence was taken and weighed. Some samples were desalinated with distilled water (0% inhibitor) to evaluate the inhibitor's effect without the dissolution effect of distilled water. The same procedures were applied to these samples as they were before.

### 2.2.2. X-ray diffraction (XRD)

Philips X-ray diffraction device model PW/1710 was used, which has a mono-chromator, Cu-radiation ( $\lambda=1.542\text{\AA}$ ) at 40Kv, 30 MA, and a scan speed of 0.02/sec. The corresponding spacing ( $d$  and  $\lambda$ ) was used to determine the reflection peaks between 2 and 60. The ICDD files are compared with the diffraction graph's relative intensities ( $1/1$ ) and relative strengths.

### 2.2.3. Scanning electron microscope attached to EDX

An SEM microscope was used to examine and analyze the painted layer. The EDX Unit that was attached to the SEM allowed Jeol JSM (5600 LV) and Philips XL 30 to obtain the micrographs. The magnification range of the EDX Unit was from 10x to 400.000x, with a resolution of  $W. is (3.5\text{nm})$ .

### 2.2.4. FTIR spectroscopy

Fourier transform infrared (FTIR) analysis was performed using the Nicolet Nexus and Nicolet Continuum. A HgCdTe detector is employed to chill the infrared spectroscopy in a microscope using liquid nitrogen ( $N_2$ ). The spectrums recorded by a Graseby-Specac diamond cell accessory in transmission mode range from 4000 to 700  $cm^{-1}$ .

### 2.2.5. Spectrophotometer

The Color EYE 3100 spectrophotometer comes equipped with a basic user manual provided by D L Company. Mineral pigment color changes were investigated through the use of primary points. To determine the E according to this equation, these points were measured both before and after treatment.

$$\Delta E^* = [(\Delta L^{*2} + \Delta a^{*2} + \Delta b^{*2})^{1/2}] \text{ where } \Delta L^* = L^*_{\text{treated}} - L^*_{\text{untreated}},$$

$$\Delta a^* = a^*_{\text{treated}} - a^*_{\text{untreated}}, \Delta b^* = b^*_{\text{treated}} - b^*_{\text{untreated}} (\Delta E^* = 5 =$$

human eye detection limit, HEDL). (L) denotes the coordinate of (black % white) and (a) denotes the coordinate of (green % red) and (b) denotes the coordinate of (blue % yellow).

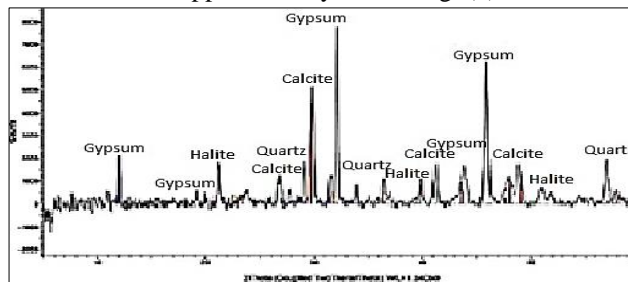
## 3. Results

### 3.1. Painted Layers morphology and structure

An ancient tomb (Amry) located in the Giza plateau, the tomb named "Emry" located in the western cemetery to the west of the Khufu Pyramid is from the Fifth Dynasty and is the burial place of "Emery, the son of Shepseskaf Ankh." His titles encompass Governor of the Great Province, Beloved of His Lord, Khufu's Priest, and Overseer of the Palace. George Reisner made the discovery in 1925. The strength and amazing painted layer of this tomb have always been lost due to the deterioration caused by salt. As per the following, small fragments were taken for analysis:

#### 3.1.1. Ground layer structure

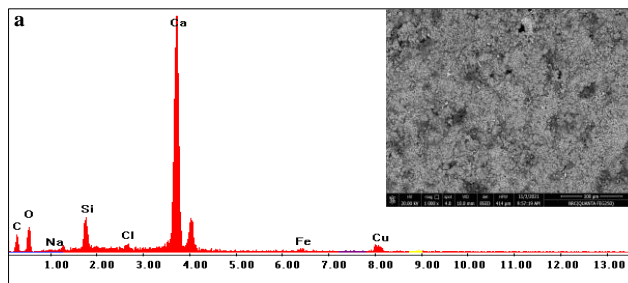
According to the XRD analysis, the ground layer is mainly composed of Gypsum ( $CaSO_4 \cdot 2H_2O$ ) at approximately 43.6%, Calcite  $CaCO_3$  at approximately 27.2%, and traces of Quartz ( $SiO_2$ ) at approximately 15.1% and Halite  $NaCl$  as a deteriorated factor of approximately 14.2%, fig. (2)



**Figure (2)** XRD pattern of the ground layer.

#### 3.1.2. Painted layer

Due to the small size of the painted layer fragments, conducting XRD analysis proved challenging. Therefore, we relied on the elements detected by EDX to infer the composition of pigments. The data of blue pigments reveals the presence of calcium (Ca), silicon (Si), and copper (Cu), which are the primary constituents of Egyptian blue ( $CaCuSi_4O_{10}$ ) fig. (3-a). The red pigment consists of Iron (Fe) and Oxygen (O), mainly Hematite ( $Fe_2O_3$ ), while Calcium (Ca), silicon (Si) are particularly indicate the ground layer fig. (3-b), the yellow pigment is composed of Iron (Fe) and Oxygen (O), Hydrogen (H) primary constituents of Goethite ( $FeOOH$ ), fig. (3-c), and the green pigment is Malachite ( $Cu_2CO_3(OH)_2$ ), according to the presence of copper (Cu), Carbon (C), Oxygen (O) and Hydrogen (H). While it is possible for the color to be Egyptian green, the fifth dynasty determined that Malachite is the appropriate choice. fig. (3-d)



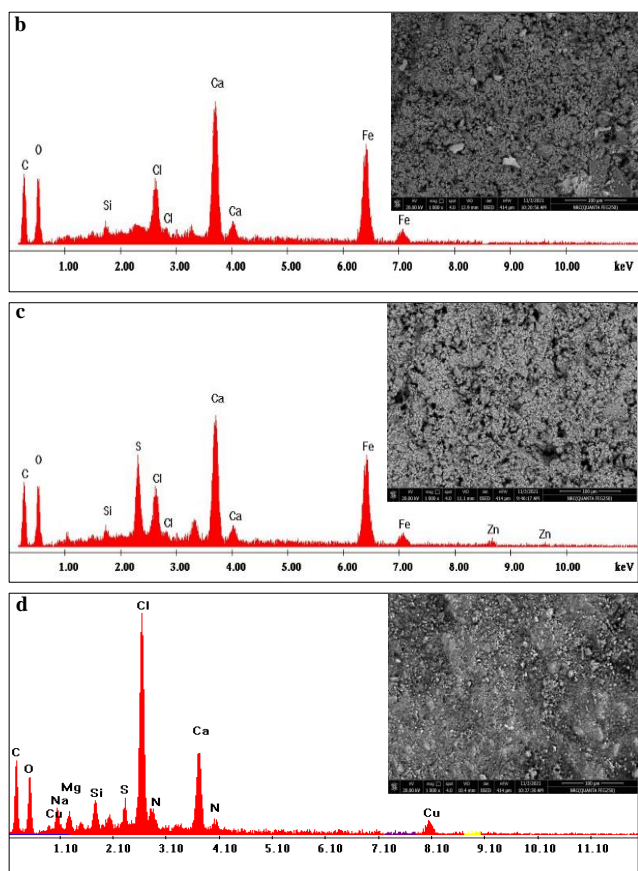


**Figure (3)** EDX spectra and SEM photomicrographs (1000 x) of **a.** the Egyptian blue, **b.** hematite, **c.** goethite, **d.** malachite

### 3.1.3. Binding medium

The binding medium was characterized by the presence of a small amount of egg yolk in the FTIR spectra. The painted layer is where the activated group can be found and is what distinguishes it, the N-H stretching at a sharp peak 3398, C-H bond at 2763, the stretching of  $-\text{CONH}_2$  in the protein is the sharp peak at 3300-3430, Amide II (CN stretching +NH bending) at  $1564\text{ cm}^{-1}$ . A peak of  $1721\text{ cm}^{-1}$  occurrence is observed in the secondary amide protein (C=O), fig. (4).

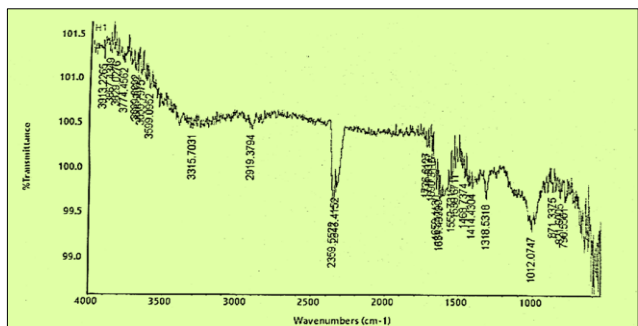


**Figure (4)** the pigment's binding medium is presented by the Egg Yolk in the FTIR spectra.

### 3.1.4. The physical properties of the replica before and after using of salt inhibitor

The physical properties of replicas were evaluated before and after 10 days of treatment, tabs, (2-a & b).

**Table (2-a)** physical properties are impacted by the use of 5M NaCl and 0M potassium ferrocyanide.

Sample	Density (g/cm <sup>3</sup> )	Water absorption %	Open Porosity %	Bulk Porosity%
1	1.12	9.06	17.23	20.1
2	1.09	9.18	17.41	20.6
3	0.93	9.21	17.50	20.00
Average	1.05	9.15	17.38	20.23

**Table (2-b)** physical properties after 10 days of using 5M NaCl and potassium ferrocyanide, the physical properties have changed.

Inhibitor KCN (M.)	Density (g/cm <sup>3</sup> )	Water absorption %	Open Porosity %	Bulk Porosity%
0%	2.11	14.62	9.18	26.83
0.01	1.00	11.14	17.44	20.29
0.1	0.97	11.68	17.52	20.54
1	0.89	13.2	17.67	20.82

### 3.2. The effect of inhibitor on the deteriorated replica

The rate of solution transportation for mural painting replicas treated with inhibitors was higher than for the control replica, particularly those treated with 1M of KCN. Salt efflorescence (shaped like a cotton flower) was the main alterations in the control sample, fig. (5-a:d). The phenomenon was visible only a couple of days after the experiment began and lasted throughout the day. The control sample fell apart on day 10, fig. (5-e & f).

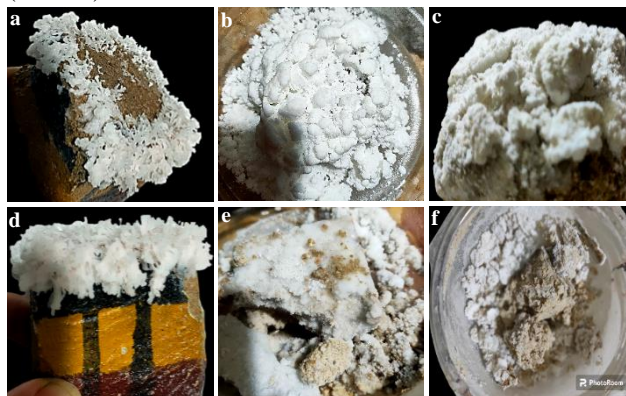


**Figure (5)** the replica undergoes crystallization of salt efflorescence during the experiment, after applying (0.01, 0.1, 1 M respectively). **a.** taken 4 days later, **b.** taken after 10 days from application (0.01, 0.1, 1M respectively), **c.** displays the salt after drying without undergoing crystallization, **d.** the pigment surfaces with salt inhibitors do not undergo crystallization; collapsed control sample after **f.** 10 days, **g.** 20 days.

### 3.3. Salt distribution in the replica

The upper section of the replica showed a significant increase in salt crystallization for a 21-day duration with the application of 1M KCN. In contrast, a substantial increase was noted for 15 days with 0.1M KCN, while the use of 0.01M KCN is permissible for a duration of 10 days. The salt assumed the look of a cotton flower. Specific days contributed to the stabilization of this saline layer. The replica may be obstructed, and there remained a residual quantity of salt solution in the crystallization dish for both 0.01M and 0.1M concentrations. The surface pigments and the uppermost region were solidified by a dense crust layer in a control replica. The SEM photomicrographs in fig. (6) and the stereomicroscope images in fig. (7) demonstrate that the crystallization type markedly differs from the cubic crystallization of normal sodium chloride

ystals. The replica salt dispersion was examined by slicing and assessing the salt distribution at varying depths, incremented by 0.5 cm, utilizing ultrasonic velocity. fig. (8).

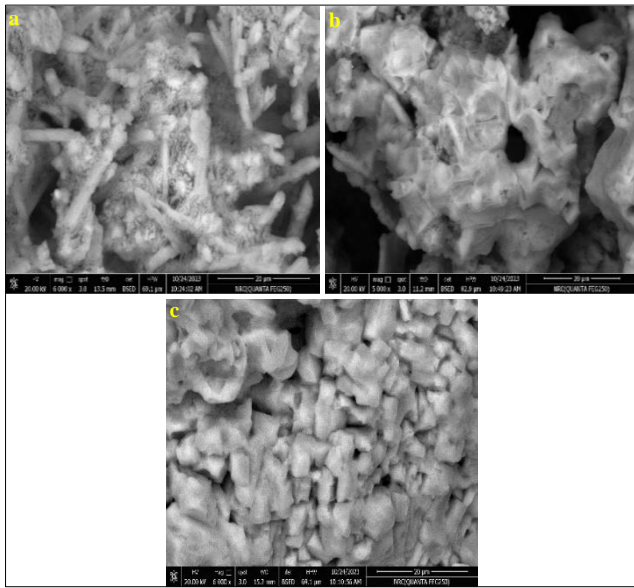


**Figure (6)** the crystallization of NaCl by salt inhibitor 6000x; **a.** 0.01M, **b.** 0.1M, **c.** 1M.

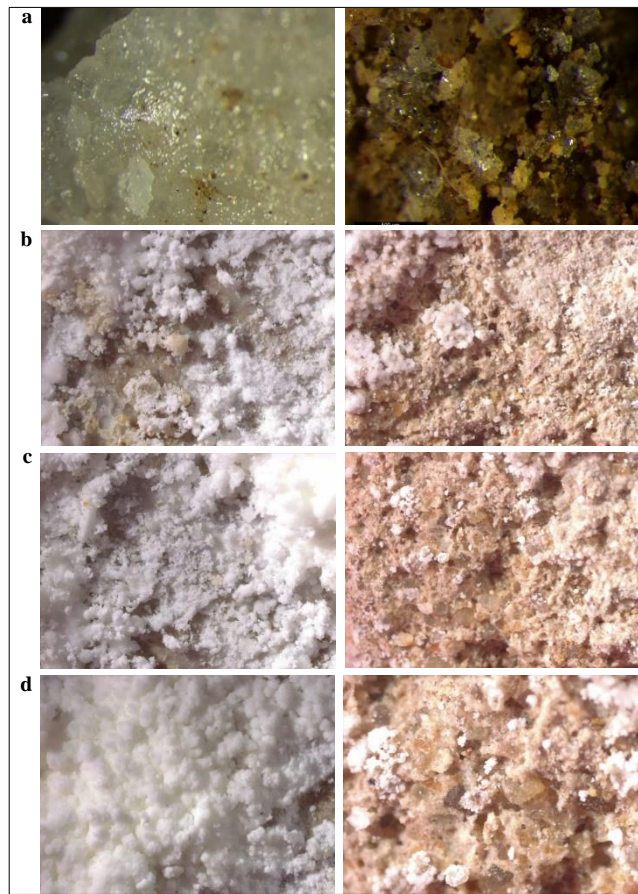


**Figure (7)** the crystallization of NaCl: **a.** control replica (left) upper (right) inner replicas, **b.** use of NaCl with 0.01M KCN for (L) upper (R) inner replicas, **c.** the use of NaCl with 0.1M KCN is made for (L) upper (R) inner replicas, **d.** the use of NaCl with 1M KCN is made for (L) upper (R) inner replicas respectively

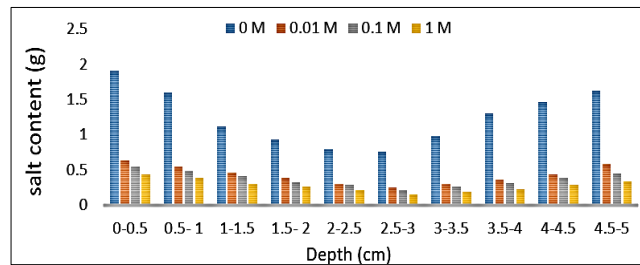


**Figure (8)** the salt distribution with/without KCN after 12 days.

### 3.4. Drying and salt content

The drying rate of the crystallization process can be accelerated by salt inhibitors via advection. Replicas containing inhibitor solution and salts exhibited a drying rate superior to those composed only of salts, fig. (9). The kinetic behavior of the evaporation rate of salt solutions within the replicas and the crystal structure of salts transitions from cubic to dendritic, likely due to the presence of potassium ferrocyanide. Salt solutions can reach the surface of mural painting replicas via benign efflorescence instead of detrimental sub-efflorescence. The efflorescence that developed on the surface of the replicas was collected and weighed following the completion of the drying process. Table (3) exhibits the efflorescence that develops on the stone surface after the drying process concludes. During the first stage of drying after inhibitor treatment, efflorescence begins to form on the replica surface, A calculation model was created using a special computer program in Excel using ultrasonic velocity, as showed before in fig. (4-f & g).

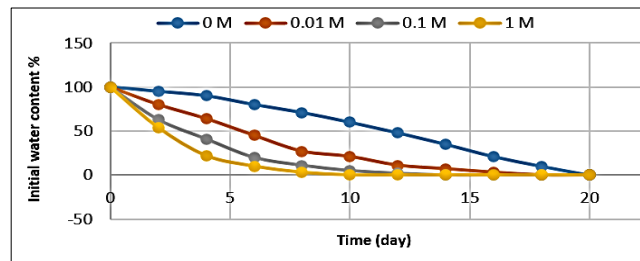


**Figure (9)** the drying curve of replica with /without KCN after 12 days.

**Table (3)** the impact of KCN on the total removability of NaCl from replica (after 12 day)

Inhibitor KCN Conc.	Initial salt content (g)	Efflorescence's formation (g)	Total removability %
0%	10.33	12.03	30.56
0.01	5.66	17.36	49.33
0.1	4.65	19.22	52.77
1	3.21	21.12	53.16

### 3.5. Color change by spectrophotometer

The color change assessment allowed to distinguish the differences between treated and untreated replicas and between each treatment concentration. The quantitative values of the outcomes for concentration 0.01M are displayed in tab. (4-a), for concentration 0.1M are displayed in tab. (4-b), and for concentration 1M are displayed in tab. (4-c).

**Table (4-a)**  $\Delta E$  of the painted layer before and after applied 0.01M potassium ferrocyanide.

Pigments	Untreated			Treated with 0.1M			$\Delta E$
	$L^*$	$a^*$	$b^*$	$L^*$	$a^*$	$b^*$	
Egyptian blue	40.65	-6.04	-20.79	39.97	-8.5	-19.47	2.87
Malachite	57.3	-10.01	6.23	57.48	-9.86	8.36	2.14
Hematite	47.46	3.87	4.02	48.02	4.66	4.77	1.22
Goethite	54.69	8.16	13.07	52.38	7.51	1.98	1.32

**Table (4-b)**  $\Delta E$  of the painted layer before and after applied 0.1M potassium ferrocyanide.

Pigments	Untreated			Treated with 1M			$\Delta E$
	$L^*$	$a^*$	$b^*$	$L^*$	$a^*$	$b^*$	
Egyptian blue	40.65	-6.04	-20.79	38.33	-10.37	-17.99	5.65
Malachite	57.3	-10.01	6.23	59.96	-11.81	7.59	3.49
Hematite	47.46	3.87	4.02	48.21	5.56	5.38	2.3
Goethite	54.69	8.16	13.07	55.29	7.41	13.98	2.25

**Table (4-c)**  $\Delta E$  of the painted layer before and after applied 1M potassium ferrocyanide.

Pigments	Untreated			Treated with 1M			$\Delta E$
	$L^*$	$a^*$	$b^*$	$L^*$	$a^*$	$b^*$	
Egyptian blue	40.65	-6.04	-20.79	37.14	-11.02	-15.98	8.6
Malachite	57.3	-10.01	6.23	64.91	-9.72	8.33	7.9
Hematite	47.46	3.87	4.02	49.36	6.46	6.11	3.86
Goethite	54.69	8.16	13.07	55.93	7.11	14.11	2.44

#### 4. Discussion

Salt crystallization has consistently caused the degradation of an ancient tomb (Emry) located on the Giza plateau. The ground layer was analyzed using XRD. The data indicated that the composition included gypsum ( $\text{CaSO}_4 \cdot 2\text{H}_2\text{O}$ ), calcite ( $\text{CaCO}_3$ ), and trace amounts of quartz ( $\text{SiO}_2$ ), which were damaged by halite ( $\text{NaCl}$ ). [29,30]. The diminutive size of the painted layer particles rendered XRD analysis difficult. Consequently, we utilized the elements identified by EDX to deduce the composition of pigments. The analysis of blue pigments indicates the presence of calcium (Ca), silicon (Si), and copper (Cu), which are the principal components of Egyptian blue. The red pigment comprises iron (Fe) and oxygen (O), predominantly Hematite, the yellow pigment consists of Iron (Fe), oxygen (O), and hydrogen (H), primarily forming goethite and the green pigment is malachite indicated by the presence of copper (Cu), carbon (C), oxygen (O), and hydrogen (H). These pigments were used in the old Kingdom as the tomb belongs to it (5<sup>th</sup> dynasty) [3,31]. The FTIR spectrum of egg yolk was the basis for characterizing the binding medium. Amide II (CN stretching +NH bending) takes place at  $1564 \text{ cm}^{-1}$  and the N-H stretching occurs at a sharp peak of  $3398 \text{ cm}^{-1}$ , while the C-H bond takes place at  $2763 \text{ cm}^{-1}$ . The secondary amide protein C=O has been observed to be at a peak of  $1721 \text{ cm}^{-1}$  [32,33]. According to prior data, mortar specimens (replicas) are often manufactured on stone (the exterior wall of the tomb), utilizing filter paper as a separator between the stone and the ground layer. The tomb was originally constructed to permit moisture to permeate through the mortar and stone, resulting in a realistic porosity and pore size in the mortar specimens (Replica). The specimens were colored, and their physical properties were examined before and after a 10-day consumption of potassium ferrocyanide. A high concentration of potassium ferrocyanide enhances both open and bulk porosity. The translocation of salt from the internal pores to the surface may lead to that occurrence. Efflorescence prevents the pores of the replica from being obstructed, facilitating the migration of excess salts from the pores to the drying surface [34]. The cyanide product as sodium cyanide facilitates the movement of salt from the inner pores to the surface without inflicting additional harm; however, it unfortunately results in significant color alteration, particularly affecting white pigments. [26,35]. For porous materials, this effect enables potassium and sodium ferrocyanide to decrease the evaporation rate of the salt solution within the pore structure of the

stone and facilitates the crystallization of NaCl and KCl on the stone's surface as efflorescence rather than subflorescence. [8,36]. As the capillary's water absorption rises, a greater quantity of salt crystals dissolves. Conversely, it diminishes the density that may necessitate consolidation as the next phase. [37]. The salt crust induces detachment of the replica components, leading to flaking, scaling, and granular disintegration. If the mural paintings are highly delicate, the salt crust will disintegrate into a powder consequently. Moreover, the salt crust can inhibit water vapor diffusion by obstructing the surface of the replica. [33,38]. During the salt distribution testing of the replica, a certain day resulted in the stabilization of the salt layer. The replica may be obstructed, and residual salt solution remained in the crystallization dish at both 0.01M and 0.1M concentrations. In a controlled replica case, a dense crust layer solidified the surface pigments and the upper area. The conventional sodium chloride crystal exhibited a cubic crystallization distinct from this specimen. The concentration of salts in the replicas is diminished by the descending effect of efflorescence salt [39]. The pores in the stone are prevented from being obstructed by efflorescence, which allows the movement of additional salts from within the stone to the drying surface. By acting like a saturated network with a very high surface area and greater surface area for evaporation, Efflorescence significantly increases the evaporation rate. The use of inhibitors resulted in a significant increase in the rate of evaporation due to the decrease in surface tension of the salt solution. The capillary pressure in a pore radius decreased, resulting in a faster evaporation rate [22,40]. This method was employed to evaluate the distribution of salt inside the samples before and after treatment with a crystallization inhibitor. This technique leads to the creation of innocuous efflorescence rather than detrimental sub-florescence. Efflorescence diminishes the salt concentration in replica mural paintings by acting as a salt drain [41]. Efflorescence formation maintains the pores in the replica unobstructed, facilitating the transfer of supplementary salts from the pores to the drying surface [34]. The findings indicate that potassium ferrocyanide significantly affects nucleation. The measurements from the spectrophotometer provide the foundation for this. The  $L^*$  value diminished due to the elevated (1M) concentration of potassium ferrocyanide. The reduction in  $b^*$  value resulted in a darkening and a transition toward blue. This outcome results from the visible link between Egyptian blue and malachite [42]. Low concentrations resulted in a color shift within range of the commonly accepted threshold for conservation treatments ( $E^* = 5$ ) [43]. While sodium ferrocyanide is useful as a salt inhibitor, we prefer potassium ferrocyanide for several reasons, namely its lower toxicity, particularly at low concentrations. The release of sodium ions during the reaction of sodium ferrocyanide may enhance the creation of NaCl due to its reaction with chlorine present in the soil, which is reactive. Salt inhibitors do not function as a primary treatment; instead, they provide protection against more damage. Consequently, prior to the use of salt inhibitors, it is essential to eliminate the substantial crystallization salts utilizing a poultice (by diffusion or advection). Subsequently, we can employ salt inhibitors to prevent the re-crystallization of salt. Furthermore,

it may be essential to solidify the object post-treatment. Conversely, the novel creation of salt crystallization following treatment with inhibitors is less detrimental to the painted layer, since the new formations will naturally descend due to gravity force without inflicting more harm, and the cubic halite is less substantial due to its dendritic morphology.

## 5. Conclusion

The aim of this research is to evaluate the efficacy and compatibility of Potassium ferrocyanide as a salt inhibitor for mural paintings. Two techniques were employed for the procedures: injection and brushing. The study demonstrates the efficacy of potassium ferrocyanide-as salt inhibitor on replicas of mural paintings. The impact is typically more refined at 0.01M and 0.1M KCN compared to 1M KCN due to the sensitivity of blue and green pigments. The upper layer had a higher concentration of salt compared to the middle layer. Increased concentrations of potassium ferrocyanide result in heightened values of both open and bulk porosity. The production of efflorescence assists in the clearing of replica pores, therefore promoting the movement of salt from internal pores to the surface. Research indicates that the color change following the addition of 0.01M and 0.1M KCN generally remains out the detection range of the human eye. The desalination rate is considerably influenced by 1M Potassium ferrocyanide, which also results in the darkening of Egyptian blue and Malachite pigments. Further research should be conducted in the future to determine the cause of the darkness in copper-based pigments. Is it attributable to the creation of copper ferrocyanide or not? That which should be identified in the future. The low concentration of potassium ferrocyanide makes it effective and non-toxic; yet, a concentration of 1M leads to significant color change. The protection of harm crystallization of salts in ancient pigment layers can be achieved using potassium ferrocyanide, a highly effective salt inhibitor.

## References

- [1] Goudie, A. & Viles, H. (1997). *Salt weathering hazards*, Wiley & Sons, UK.
- [2] Charola, A. & Bläuer, C. (2015). Salts in masonry: An overview of the problem. *Restor. Build. Monum.* 21: 119-135.
- [3] El Goresy, A., Jaksch, H., Razeq, M., et al. (1986). Ancient pigments in wall paintings of Egyptian tombs and temples: An Archaeometric Project. Rep MPIHV, Vol. 12, <https://api.semanticscholar.org/CorpusID:192184648> (5/10/2024)
- [4] Nijland, T., Adan, O., Van Hees, R., et al. (2009). Evaluation of the effects of expected climate change on the durability of building materials with suggestions for adaptation. *Heron.* 54: 37-48.
- [5] Brachaczek, W. (2013). The hydrophobicity of renovation plaster in manufacturing technology optimized by statistical methods. *Constr. Build. Mater.* 49: 575-582.
- [6] EL Hagrassy, A. (2010). *Study for treatments the effect of the microbiological deterioration of mural painting executed by Tempra technique, applied on selected models, (Derasa le elag ta'ther el talaf el microbiology ala el sewar el gedarya almonafza be oslob el tempra tatbeka ala namozag mokhtar)*, MA Faculty of archaeology, Cairo Univ., Egypt.
- [7] Shen, Y., Linnow, K. & Steiger M. (2020). Crystallization behavior and damage potential of Na<sub>2</sub>SO<sub>4</sub>-NaCl mixtures in porous building materials. *Crystal Growth & Design.* 20: 5974-5985.
- [8] Rodríguez-Navarro, C. & Doehne, E. (1991). Salt weathering: Influence of evaporation rate, supersaturation and crystallization pattern. *Earth Surface Processes and Landforms.* 24: 191-269.
- [9] Steiger, M. (2005). Crystal growth in porous materials: The crystallization pressure of large crystals. *J. of Crystal Growth.* 282: 455-469.
- [10] EL Hagrassy, A. (2022). *Tricoderma spp.* in cultural heritage mural paintings of ancient tomb, their antifungal and bioactivity. *JGUAA.* 2 (7/2): 165-183.
- [11] Abu Alhassan, Y. (2024). Laboratory investigation of sodium ferrocyanide as a crystallization inhibitor to prevent the destruction of rock-cut monuments in Petra – Jordan due to the attack of salt mixtures, *EJARS.* 14 (1): 43-49
- [12] Brachaczek, W. (2021). Renovation of buildings having damp and salted walls- case analysis. *Acta Sci. Pol. Architectura.* 20: 51-64
- [13] Ottosen, M. & Dalgaard, I. (2009). Desalination of a brick by application of an electric DC field. *Mater. Struct.* 42: 961-971.
- [14] Fragata, A., Veiga, M. & Velosa, A. (2016). Substitution ventilated render system for historic masonry: Salt crystallization tests evaluation, *Construction & building Materials.* 102 (1): 592-600.
- [15] Falchi, L., Zendri, E., Capovilla, E., et al. (2017). The behaviour of water-repellent mortars with regards to salt crystallization: From mortar specimens to masonry/ render systems. *Materials & Structures.* 50 (1): 50-66.
- [16] Fragata, A., Veiga, R. & Velosa, A. (2021). Performance of a salt-accumulating substitution lime render for salt laden historic masonry walls. *Heritage.* 4: 3879-3891.
- [17] Groot, C., Van Hees, R., Wijffels, T., et al. (2004). Aspects of salt and moisture transport in restoration plasters and renders. *Restoration of Buildings & Monuments.* 10 (6): 593-608
- [18] Foraboschi, P. & Vanin, A. (2014). Experimental investigation on bricks from historical Venetian buildings subjected to moisture and salt crystallization. *Engin. Failure Anal.* 45: 185-203.
- [19] El-Gohary, M. (2012). Behavior of treated and un-treated lime mortar before and after artificial weathering. *Restoration of Buildings & Monuments.* 18 (6): 369-380
- [20] Sangwal, K. (1993). Effect of impurities on the processes of crystal growth. *J. Cryst. Growth.* 128: 1236-1244.
- [21] Sangwal, K. (1998). Growth kinetics and surface morphology of crystals grown from solutions: Recent observations and their interpretations. *Prog. Cryst. Growth Charact.* 36: 163-248.
- [22] Rodríguez-Navarro, C., Linares-Fernandez, L., Doehne, E., et al. (2002). Effects of ferrocyanide ions on NaCl crystallization in porous stone. *J. of Crystal Growth.* 243: 503-516.
- [23] Hutter, J., Hudson, S., Smith, C., et al. (2004). Banded crystallization of tricosane in the presence of kinetic inhibitors during directional solidification. *Cryst. Growth.* 273: 292-302.
- [24] Hernandez, A., Rocca, A., Power, H., et al. (2006). Modelling the effect of precipitation inhibitors on the crystallization process from well mixed over-saturated solutions in gypsum based on Langmuir-Volmer flux correction. *Cryst. Growth.* 295: 217-230.

- [25] Bode, A., Vonk, V., Bruele, F., et al. (2012). Anticaking activity of ferrocyanide on sodium chloride explained by charge mismatch. *Crystal Growth & Design*. 12: 1919-1924.
- [26] Lubelli, B. & Van Hees, R. (2007). Effectiveness of crystallization inhibitors in preventing salt damage in building materials. *J. of Cultural Heritage*. 8: 223-234.
- [27] Selwitz, C. & Doehne, J. (2002) The evaluation of crystallization modifiers for controlling salt damage to limestone. *J. of Cultural Heritage*. 3 (3): 205-216
- [28] Sen, A. & Ganguly, B. (2013). Is dual morphology of rock-salt crystals possible with a single additive? The answer is yes, with barbituric acid, *Angewandte Chemie-Int. Edition*. 51: 11279-11283.
- [29] Lucas, A. (1962). *Ancient Egyptian materials and industries*. 4<sup>th</sup> ed. Rev. J.R. Harris. Edward Arnold, London.
- [30] Uda, M. (2004). In situ characterization of ancient plaster and pigments on tomb wall in Egypt using energy dispersive X-ray diffraction and fluorescence. *Nuclear Instruments and Methods in Physics Research B*. 226: 75-82
- [31] Russell, W. (1893-4). Ancient Egyptian pigments. *Nature*. 49: 374-375.
- [32] Ganesan, P. & Benjakul, S. (2010). Influence of different cations on chemical composition and microstructure of pidan white and yolk during pickling and aging. *Int. J. of Food Properties*. 13: 1150-1160.
- [33] Ganesan, P., Benjakul, S. & Baharin, B. (2014). Effect of different cations in pickling solution on FTIR characteristics of pidan white and yolk in comparison to the fresh duck egg. *Sains Malaysiana*. 43: 1883-1887.
- [34] Gupta, S. (2013). *Sodium chloride crystallization in drying porous media: Influence of inhibitor*, PhD, Applied Physics dept., Eindhoven Univ. of Technology, Netherlands.
- [35] Gupta, S., Terheiden, K., Pel, L., et al. (2012). Influence of ferrocyanide inhibitors on the transport and crystallization processes of sodium chloride in porous building materials. *Crystal Growth and Design*. 12 (8): 3888-3898.
- [36] Benavente, D., Cura, M., Guinea, J., et al. (2004). Role of pore structure in salt crystallization in unsaturated porous stone. *J. of Crystal Growth*. 260: 532-544.
- [37] Nunes, C., Maria Aguilar Sanchez, A., Godts, S., et al. (2021). Experimental research on salt contamination procedures and methods for assessment of the salt distribution. *Construct. Build. Mater*. 298, doi: 10.1016/j.conbuildmat.2021.123862 23862.
- [38] Saleh, M., Darwish, S. & Elzoghby, M. (2022). The effectiveness of some crystallization inhibitors in preventing salt damage to limestone. *J. of Crystal Growth*. 585, doi: 10.1016/j.jcrysgro.2022.126606.
- [39] Cardinali, F., Bracciale, M., Santarelli, M., et al. (2021). Principal component analysis (PCA) combined with naturally occurring crystallization inhibitors: An integrated strategy for a more sustainable control of salt decay in built heritage. *Heritage*. 4: 220-229.
- [40] Espinosa-Marzal, R. & Scherer, G. (2010). Mechanisms of damage by salt, Limestone in the Built Environment: Present- decay challenges for the preservation of the past. In: Smith, B., Gomez-Heras, M., Viles H., et al. (eds.) *Geological Society*, London, pp. 61-78.
- [41] Rivas, T., Alvarez, E., Mosquera, M., et al. (2010). Crystallization modifiers applied in granite desalination: The role of the stone pore structure. *Construction & Building Materials*. 24: 766-776.
- [42] Bratitsi, M., Liritzis, I., Vafiadou, A., et al. (2018). Critical assessment of chromatic index in archaeological ceramics by Munsell and RGB: Novel Contribution to characterization and Provenance Studies. *MAA*. 18: 175-211.
- [43] Atodiresei, G., Sanddu, I., Tulbure, E. et al. (2013). Chromatic characterization in Cielab system for natural dyed materials, prior activation in atmospheric plasma type DBD. *Revista de Chimie*. 64: 165-169